v. 3, n. 4, 2023

International Journal of Biological and Natural Sciences

THE MICRORNA-137 WAS PREDICTED TO REGULATE THE MITOGEN-ACTIVATED PROTEIN KINASES AND PLURIPOTENCY-RELATED PATHWAYS IN THE MDA-MB-231 CELLS

Ruth Ruiz Esparza-Garrido
Investigadora por México, Non-coding RNAs Laboratory, Medical Research Unit on Human Genetics, Children's Hospital" Silvestre Frenk Freund", National Medical Center Century XXI, Instituto Mexicano del Seguro Social (IMSS).

Andrea Viridiana Cervantes Ayala
Non-coding RNAs Laboratory, Medical Research Unit on Human Genetics, Children's Hospital "Silvestre Frenk Freund", National Medical Center Century XXI, Instituto Mexicano del Seguro Social (IMSS).

Miguel Ángel Velázquez-Flores
Non-coding RNAs Laboratory, Medical Research Unit on Human Genetics, Children's Hospital "Silvestre Frenk Freund", National Medical Center Century XXI, Instituto Mexicano del Seguro Social (IMSS).

All the authors declare no conflict of interest

Abstract: Breast cancer represents one of the main causes of mortality in Mexico and in the world and at present, efforts have been made to identify possible biomarkers to improve the diagnosis and prognosis of this group of diseases. BIK (BLC2-Ibnteracting Killer), a protein involved in the regulation of apoptosis, has been identified to interact with the MDA-MB-231 cells genome, including the genomic region of microRNA-137. Accordingly, the aim of this work was to characterize the expression of miR-137 and begin to identify the function of BIK in the MDA-MB-231 cells. The mRNA expression of epithelial and mesenchymal MDA-MB-231 cells markers and that of miR-137 and BIK was studied by qPCR. The biological pathways potentially regulated by the miR-137 were predicted with the DIANA-miRPAth database. Epithelial and epithelial-mesenchymal transition markers showed the expression previously reported for the MDA-MB-231 cells. Meanwhile, the expression of the miR-137 was 3 ± 0.02-fold lower in the MDA-MB-231 cells than in the HMEC cells and conversely, BIK expression increased by 0.66 ± 0.13 in contrast to HMEC. Bioinformatic predictions showed that the miR-137 target genes (predicted and validated) were mainly involved in the mitogen-activated protein kinases pathway and in pathways regulating stem cell pluripotency. In conclusion, our data showed that MDA-MB-231 cells have the molecular features previously reported for this cell line; the miR-137 downregulation could be related to the malignancy of the MDA-MB-231 cells, by regulating signaling pathways related to cancer.

Keywords: Cancer. MDA-MB-231. micro-RNAs. miR-137. BIK. Oncogene.

INTRODUCTION

Breast cancer (BC) represents one of the main challenges in public health, as it is one of the main causes of mortality in women in Mexico and the world **(1)**. One of the main clinical challenges is the early detection and proper molecular classification of BC for the application of the correct treatment. The MDA-MB-231 cell line has a high invasive and metastatic capacity, and recently, it was identified the physical BIK interaction with coding and noncoding regions of the MDA-MB-231 cells genome, specifically in regions where several microRNA (miRNA) genes are located, such as the MIR137HG **(2)**.

MiRNAs are small non-coding RNAs that act as regulators of gene expression at transcriptional **(3)** and post-transcriptional levels **(4)**, as well as agonist for toll receptors **(5)** and regulators for other noncoding RNAs **(6)**. Currently, aberrant changes in the expression patterns of miRNAs improved the molecular classification of mammary tumors **(7, 8)known as microRNAs (miRNAs**. Particularly, the miR-137 has been described as a tumor suppressor in several types of cancer, such as BC, melanoma, osteosarcoma, pediatric gliomas, tongue, lung, ovarian, thyroid, and gastric cancer **(9-14)aurora kinase A (AURKA**, and as oncogene in specific BC cell lines **(15)** and in bladder cancer **(16)**. In the present study, the miR-137 and BIK expression was determined by qPCR and the signaling pathways potentially controlled by the miR-137 were predicted with the DIANA-miRPath database.

METHODS

MDA-MB-231 cell culture

The MDA-MB-231 cell line (ATCC® HTB-26™) was cultured in DMEM/F12 medium with 10% fetal bovine serum (FBS; v/v) and in the presence of 100 U/mL penicillin. Cells were maintained at 37°C with 5% CO_2.

Cell counting was carried out using the Neubauer method (Celeromics) (1). For this, cells were detached with 0.5% trypsin-EDTA and cell counting was done every 24 hours for 6 days. The percentage (%) of cell growth was calculated from three independent experiments.

RNA extraction

The MDA-MB-231 cells (65% confluence) were detached from culture plates with 0.5% trypsin-EDTA and incubated at 37°C for 10 minutes; the reaction was stopped with 1mL of fresh culture medium. Cells were then washed with 1X PBS (phosphate buffered saline: [138 mM] NaCl; [3 mM] KCl; [8.1 mM] $Na_2HPO_{4;}$ and [1.5 mM] KH_2PO_4), transferred to 1.5 mL tubes, and centrifuged at 800xg for 10 minutes, at room temperature (~25°C). The supernatant was discarded and RNA was extracted by the TRIzol™ method. Once purified, the RNA was stored at -20°C until use. Subsequently, the RNA concentration and quality was determined by spectrophotometry on the NanoDrop 1000 (ThermoScientific, USA).

cDNA synthesis

cDNA was synthesized to detect mature miRNAs and mRNAs, by means of the miScript II RT kit (Qiagen). The components of the reactions were: 4 µL of 5x miScript HiSpec Buffer (cDNA synthesis for miRNAs) or 4 µL of 5x miScript HiFlex Buffer (cDNA synthesis for mRNAs); 2µL of 10x Buffer miScript Nucleics Mix; 2µL of Buffer miScript Nucleics Mix; 2µL of miScript Reverse Transcriptase Mix; and 12µL of purified RNA (235ng). The reaction was performed following the manufacturer's recommended protocol: 37°C (60 min); 95°C (5 min). Finally, the cDNA was stored at -20°C until PCR was performed.

qPCR

The mRNAs expression was determined by using the RealQ Plus 2x Master Mix Green kit (Ampliqon). The primers were designed using the Blast program **(Table 1)** and were synthesized by T4Oligo (Guanajuato, Mexico). The reagents used for the reaction were: 10µL of RealQ Plus 2x Master Mix; 1 µL of the forward primer; 1 µL of the reverse primer; 300 ng of the cDNA template; and 6µL of RNAse-free water, for a final reaction volume of 25 µL. The reaction was performed on the StepOnePlus™ Real-Time PCR System thermal cycler (ThermoScientific, USA) under the following conditions: initial activation (95°C; 15 min); 40 cycles: 95°C (15 sec); TM° of primers (1 min). The expression of these markers was normalized with the GADPH gene.

For detection of mature miR-137, the kit miScript SYBR® Green PCR (Qiagen) was used. The reagents used for the reaction were: 2 µL of the 2x SYBR Green PCR Master Mix; 2.5 µL of the 10x miScript Universal Primer; 2.5µL of the primer for miR-137; 150 ng of the cDNA template; and 5µL of RNAse-free water, for a final reaction volume of 25 µL. The reaction was performed under the following conditions: initial activation (95°C; 15 min); 40 cycles: 94°C (15 sec); 55°C (30 sec); 70°C (30 sec). Expression was normalized with the miR-16 gene.

The relative values of expression were obtained by means of the mathematical model described by Livak and Schmittgen **(17)**. Agarose gels were run to check the expected size of the amplicons and to confirm that the reactions were specific.

PREDICTION OF MIR-137-REGULATED BIOLOGICAL PATHWAYS

The prediction of the miR-137 target genes and the potential cellular pathways regulated by this miRNA were elucidated with the

DIANA-miRPath v.3 software **(18)**, by using TaRBase v7.0 (validated genes), micro-TDS v5.0 (predicted genes), and TargetScan (predicted genes) tools. Pathways in which the value of $p<0.05$ were taken into account.

STATISTICAL ANALYSIS

The results represent the mean ± SEM of 3 independent experiments. A Shapiro-Wilk normality test and a Student's *t* test for independent samples were applied to all results. Values of $p<0.05$ were taken as significant differences. This statistical analysis was performed in the GraphPad Prism V.6 program.

RESULTS

MDA-MB-231 cells

Under our culture conditions, the MDA-MB-231 cells increased in number by 25 ± 1.4 % and 100 ± 19 % at 24 and 48hrs (0.7-fold increase versus 24 hrs), respectively. Cell growth plateaued at 144 hrs (280 ± 2 %; 0.8-fold increase versus 48 hrs) **(Figure 1A)**. In Figure 1B-F (4 days of culture), the spindle-shaped phenotype of cells is clearly distinguishable. These results are similar to the growth time reported by the American Type Culture Collection (ATCC®), which reports doubling of these cells at 38 hours and stabilization of their growth (stationary phase) at approximately 144 hours (29).

Molecular characterization of the MDA-MB-231 cells

To corroborate that the MDA-MB-231 cell line has the molecular characteristics previously described in the literature **(19)** the relative expression of some epithelial and mesenchymal molecular markers was determined. As reported, the epithelial markers CDH1 (Cadherin 1) and EPCAM (Epithelial cell adhesion molecule) showed a lower relative expression (-6 ± 0.3-fold (CDH1) and -5.7 ± 1.4-fold (EPCAM)) in the MDA-MB-231 cells relative to the non-neoplastic HMEC line **(Figure 2A)**. Meanwhile, VIM and SNAI1 showed respectively a 14 ± 5.4-fold and 9 ± 4.8-fold increase in expression in the MDA-MB-231 cells compared to HMEC **(Figure 2A)**.

MiR-137 and BIK expression

The miR-137 expression was determined by RT-qPCR. The results showed that the expression of this miRNA decreased by 3 ± 0.02-fold in the MDA-MB-231 cells compared to HMEC (1 ± 0.01) **(Figure 2B)**. By contrast, BIK expression was slightly upregulated in the MDA-MB-231 cells (0.66 ± 0.13-fold) relative to HMEC **(Figure 2C)**.

DIANA-miRPath analyses

To analyze the biological pathways potentially regulated by miR-137, the DIANA-miRPath software v.3 was used. The number of genes identified with each of the tools and the biological pathways enriched with the target genes, validated for the miR-137, are depicted in Tables 2 and 3. All validated target genes are described in **Supplementary Table S1**.

In order to have a highest predictive power, the pathways potentially regulated by this miRNA were identified from the validated and predicted genes **(Table 4; Figure 3 A, B)**. All the pathways are depicted in the **Supplementary Table S2**. According to this analysis, the mRNAs potentially regulated by miR-137 participate in signaling pathways such as the MAPK (mitogen-dependent protein kinases), ErbB (Erb-B receptor tyrosine kinase), Hippo (Hippo protein kinase), and cAMP (cyclic adenosine monophosphate), as in pluripotency-related pathways. Modifications in any of these pathways could alter cellular processes such as cell cycle, survival, cell adhesion, pluripotency and apoptosis.

DISCUSSION

Under our culture conditions, M231 cells growth similar to time reported by the American Type Culture Collection (ATCC®). The relative expression of some epithelial and mesenchymal molecular markers was determined by qPCR, showing lower levels of the epithelial markers CDH1 (Cadherin 1) and EPCAM (Epithelial cell adhesion molecule), and an increased expression of VIM and SNAI1 in the MDA-MB-231 cells compared to the non-neoplastic HMEC line. The MDA-MB-231 cell line is classified within the molecular subtype *´claudin-low'*, whose main characteristics are the low expression of genes involved in cell adhesion, such as CDH1 and EPCAM; and the high expression of mesenchymal markers such as VIM, SNAI1, TWIST1, ZEB2, and CDH2 **(19-22)**. The expression of these markers is related to the EMT process, involving the loss of epithelial markers and the gain of mesenchymal markers that induce morphological changes (by cytoskeleton remodeling) and the loss of both apical and basal polarity, as well as cell-cell adhesion. All this has as a consequence cell migration and invasion **(21-23)**.

After the characterization of the cell line, we analyzed the miR-137 expression by RT-qPCR. The expression profile of miR-137 was similar to the relatively low levels observed in different types of cancer **(9, 13, 14, 24, 26-28)**. In BC, the miR-137 expression changed according to the molecular subtype in which it is studied from approximately -3 to -40-fold. Our data correlated with those reported by Zhao et al. **(28)**, who observed low miR-137 expression in several BC cell lines, including the MDA-MB-231 cells (~45-fold decrease) compared to the MCF10A cells. Similarly, another study also found a decrease (~25-fold decrease) on the miR-137 expression in the MDA-MB-231 cells **(29)**. In contrast, relatively high miR-137 levels (~3-fold increase) were detected in mammary tumor samples (grade IV) and in the BC cell lines MCF7 (Luminal A) and BT474 (Luminal B) **(33)**. This could be due to the fact that in this study adjacent tissues were used as control tissues for comparison of miRNA expression level. Taken together, these data indicate that miR-137 expression change according to the molecular subtype of BC under study, and in particular, in the 'claudin-low' subtype this miRNA is downregulated.

In other way, the expression changes of BIK seem to affect the expression levels of mir137, because it was shown that BIK bound to the promoter region of this miRNA **(2)**. The relative BIK expression was slightly increased in the MDA-MB-231 cells compared to the HMEC cells, which is in agreement with its upregulation in BC ductal adenocarcinoma samples **(31)** and in BC cell lines **(32)**. In 2016, a paper reported that increased expression of BIK, in patient samples, was associated with poor disease prognosis, suggesting a likely activity of BIK as a tumor promoter by inducing autophagy **(33)**. The nuclear localization of BIK and its physical interaction with the genome of the MDA-MB-231 cells strongly suggest that BIK has functions other than acting as a regulator of apoptosis. Particularly, its interaction with the MIR137HG promoter region suggests that BIK regulates the expression of this miRNA by acting as a transcription factor. Therefore, BIK could have oncogenic functions in BC, despite being described as a tumor suppressor in other types of cancer **(34, 35)**.

Finally, according to what was obtained with the DIANA-miRPath software, the genes potentially regulated by the miR-137 participate in signaling pathways such as MAPK, ErbB, Hippo, and cAMP, as well as pluripotency-related pathways. Modifications in any of these pathways could

alter cellular processes such as cell cycle, survival, cell adhesion, pluripotency and apoptosis. The MAPK signaling pathway regulates important cellular processes, such as proliferation, differentiation, apoptosis, survival, inflammation, autophagy, and immunity **(36-38)**. This signaling cascade can be activated by cytokines, growth factors, and/or extracellular matrix molecules. It is composed of serine-threonine protein kinases that upon activation phosphorylate different proteins (including transcription factors), determining the cellular response **(38)**. Aberrant activation of this pathway represents an oncogenic event of major importance in the development and progression of multiple types of cancer **(36)**. Mutations or changes in the expression of upstream and downstream regulators are frequent. For example, the RAS-MAPK pathway is altered in 67% of cases of T-cell precursor acute lymphoblastic leukemia, and the aberrant activation of the RAS-RAF-MEK-ERK-MAPK pathway has been observed in different types of BC **(39)**.

Cancer trochlear cells (CSCs) are a small group of cells with the ability to self-renew and produce differentiated cancer cells **(40, 41)**. What differentiates CSCs from embryonic stem cells (ESCs), is that the former lose control of replication and differentiation, leading to tumorigenesis **(41)**. CSCs are responsible for initiating and sustaining tumor growth, as well as for carrying out the process of metastasis **(42)**. Transcription factors and signaling pathways that regulate ESCs stemness also play important roles in the maintenance of CSCs **(43)**. Among the most important transcription factors are Sox2 (SYR Box 2), whose deregulated expression was observed in different types of cancer, such as brain tumors, lung, colon, and BC **(40)**, Klf4 (Kruppel-like factor 4), whose target genes are involved in cell cycle control and which depending on the type of cancer acts as a tumor suppressor (gastric and colon cancer) or as an oncogene (breast and skin cancer) **(40)**, and Nanog (Nanog homeotic box), which is related to the processes of renewal, proliferation, and pluripotency. The main pluripotency pathways are JAK/STAT, Wnt/β-catenin, and Sonic Hedgehog (Shh) pathway.

In hepatic CSCs, low miR-137 expression was associated with increased sphere formation and increased expression of cancer stem cell-related markers (CD133, CD44 and EpCAM) **(43)**. In the present work, some of the genes involved in pluripotency-related pathways were predicted to be potential miR-137 targets **(Figure 3B)**. Taking into account the study in hepatic CSCs and the results of the bioinformatics analysis performed here, the determination of the role of miR-137 in the maintenance of pluripotency in BC cells could help to have better information about tumor origin and progression.

CONCLUSIONS

The miR-137 expression was down-regulated in the MDA-MB-231 cells and this might be related to changes in the MAPK pathway and in pathways related to the pluripotency control.

REFERENCES

1. Sung H, Ferlay J, Siegel RL, Laversanne M, Soerjomataram I, Jemal A, Bray F. Globocan Cancer Statistics 2020: GLOBOCAN Estimates of Incidence and Mortality Worldwide for 36 Cancers in 185 Countries. CA Cancer J Clin. 2021;71(3):209-249.

2. Ruiz Esparza-Garrido R, Ayala K, Rodríguez-Corona JM, Velázquez-Flores MÁ. Accurate Identification of BIK Binding Sites at the MDA-MB-231 Cell Genome by Human Tiling Arrays. Cancer Biol Ther Oncol. 2018;2(1):1-10.

3. Liu H, Lei C, He Q, Pan Z, Xiao D, Tao y. Nuclear functions of mammalian MicroRNAs in gene regulation, immunity and cancer. Mol Cancer. 2018;17(1):64.

4. Fabian MR, Sonenberg N, Filipowicz W. Regulation of mRNA Translation and Stability by microRNAs. Annu Rev Biochem. 2010;79(1):351-379.

5. Zitzer NC, Garzon R, Ranganathan P. Toll-Like Receptor Stimulation by MicroRNAs in Acute Graft-vs.-Host Disease. Front Immunol. 2018;9:1-7.

6. Leucci E, Patella F, Waage J, Holmstrom K, Lindow M, Porse Bo, Kauppinen S, Lund AH. MicroRNA-9 targets the long non-coding RNA MALAT1 for degradation in the nucleus. Sci Rep. 2013;3:1-6.

7. Lu J, Getz G, Miska EA, Varez-Saavedra E, Lamb J, Peck D, et al. MicroRNA expression profiles classify human cancers. Nature. 2005;435(7043):834–8.

8. Iorio M V., Ferracin M, Liu CG, Veronese A, Spizzo R, Sabbioni S, et al. MicroRNA gene expression deregulation in human breast cancer. Cancer Res. 2005;65(16):7065-70.

9. Chang X, Zhang H, Lian S, Zhu W. miR-137 suppresses tumor growth of malignant melanoma by targeting aurora kinase A. Biochem Biophys Res Commun. 2016;475(3):251-6.

10. Li X, Chen W, Zeng W, Wan C, Duan S, Jiang S. microRNA-137 promotes apoptosis in ovarian cancer cells via the regulation of XIAP. Br J Cancer. 2017;116(1):66-76.

11. Chen R, Zhang Y, Zhang C, Wu H, Yang S. miR-137 inhibits the proliferation of human non-small cell lung cancer cells by targeting SRC3. Oncol Lett. 2017;13(5):3905-11.

12. Du Y, Chen Y, Wang F, Gu L. miR-137 plays tumor suppressor roles in gastric cancer cell lines by targeting KLF12 and MYO1C. Tumour Biol. 2016;37(10):13557-69.

13. Feng Q, Wu Q, Liu X, Xiong Y, Li H. MicroRNA-137 acts as a tumor suppressor in osteosarcoma by targeting enhancer of zeste homolog 2. Exp Ther Med. 2017;13(6):3167-74.

14. Sun L, Liang J, Wang Q, Li Z, Du Y, Xu X. MicroRNA-137 suppresses tongue squamous carcinoma cell proliferation, migration and invasion. Cell Prolif. 2016;49(5):628-35.

15. Ying X, Sun, Y, He P. MicroRNA-137 inhibits BMP7 to enhance the mesenchymal transition of breast cancer cells. Oncotarget. 2017;8(11): 18348– 18358.

16. Xiu Y, Liu Z, Xia S, Jin C, Yin H, Zhao W, Wu Q. MicroRNA-137 upregulation increases bladder cancer cell proliferation and invasion by targeting PAQR3. PLoS ONE. 2014;9(10): 1–7.

17. Livak KJ, Schmittgen TD. Analysis of Relative Gene Expression Data Using Real-Time Quantitative PCR and the 2-ΔΔΔCT Method. Methods. 2001;25(4):402-8.

18. Vlachos IS, Zagganas K, Paraskevopolou MD, Georgakilas G, Karagkouni D, Vergoulis T, Dalamagas T, Hatzigeorgiou AG. DIANA-miRPath v3.0: deciphering micrRNA fucntion with experimental support. Nucleic Acids. 2015;43:W460-W466.

19. Cahall CF, Lilly JL, Hirschowitz EA, Berron BJ. A Quantitative Perspective on Surface Marker Selection for the Isolation of Functional Tumor Cells. Breast Cancer (Auckl). 2015;9(Suppl 1):1-11.

20. Holliday DL, Speirs V. Choosing the right cell line for breast cancer research. Breast Cancer Res. 2011;215(13):1-7.

21. Prat A, Parker JS, Karginova O, Fan C, Livasy C, Herschkowitz JI, et al. Phenotypic and molecular characterization of the claudin-low intrinsic subtype of breast cancer. Breast Cancer Res. 2010;12(5).

22. Wei Z, Shan Z, Shaikh ZA. Epithelial-mesenchymal transition in breast epithelial cells treated with cadmium and the role of Snail. Toxicol Appl Pharmacol. 2018;344:46-55.

23. Mendez MG, Kojima S-I, Goldman RD. Vimentin induces changes in cell shape, motility, and adhesion during the epithelial to mesenchymal transition. FASEB J. 2010 Jun;24(6):1838-51.

24. Luo C, Tetteh PW, Merz PR, Dickes E, Abukiwan A, Hotz-Wagenblatt A, et al. miR-137 Inhibits the Invasion of Melanoma Cells through Downregulation of Multiple Oncogenic Target Genes. J Invest Dermatol. 2013;133(3):768-75.

25. Dong P, Xiong Y, Watari H, Hanley SJB, Konno Y, Ihira K, et al. MiR-137 and miR-34a directly target Snail and inhibit EMT, invasion and sphere-forming ability of ovarian cancer cells. J Exp Clin Cancer Res. 2016;35(132):1-9.

26. Li H, Li Y, Li Y, Shi X, Chen H. Circulating microRNA-137 is a potential biomarker for human glioblastoma. Eur Rev Med Pharmacol Sci. 2016;20:3599-604.

27. Luo Y, Li X, Dong J, Sun W. microRNA-137 is downregulated in thyroid cancer and inhibits proliferation and invasion by targeting EGFR. Tumor Biol. 2016;37(6):7749-55.

28. Zhao Y, Li Y, Lou G, Zhao L, Xu Z, Zhang Y, et al. MiR-137 targets estrogen-related receptor alpha and impairs the proliferative and migratory capacity of breast cancer cells. PLoS One. 2012;7(6).

29. Denis H, Van Grembergen O, Delatte B, Dedeurwaerder S, Putmans P, Calonne E, et al. MicroRNAs regulate KDM5 histone demethylases in breast cancer cells. Mol BioSyst. 2016;12(2):404-13.

30. Ying X, Sun Y, He P. MicroRNA-137 inhibits BMP7 to enhance the mesenchymal transition of breast cancer cells. Oncotarget. 2017;8(11):18348-58.

31. García N, Salamanca F, Astudillo-de la Vega H, Curiel-Quesada E, Alvarado I, Peñaloza R, et al. A molecular analysis by gene expression profiling reveals Bik/NBK overexpression in sporadic breast tumor samples of Mexican females. BMC Cancer. 2005;5(93):1-11.

32. Martinez-Damas MG. Determination of BIK protein expression in breast cancer cell lines MDA-MB-231 and MCF-7. Master´s Thesis. Instituto Politécnico Nacional; 2012.

33. Pandya V, Glubrecht D, Vos L, Hanson J, Mackey J, Hugh J, et al. The pro-apoptotic paradox: the BH3-only protein Bcl-2 interacting killer (Bik) is prognostic for unfavorable outcomes in breast cancer. Oncotarget. 2016;7(22).

34. Sturm I, Stephan C, Gillissen B, Siebert R, Janz M, Radetzki S, et al. Loss of the tissue-specific proapoptotic BH3-only protein Nbk/Bik is a unifying feature of renal cell carcinoma. Cell Death Differ. 2006;13(4):619-27.

35. Arena V, Martini M, Luongo M, Capelli A, Larocca LM. Mutations of the BIK gene in human peripheral B-cell lymphomas. Genes Chromosom Cancer. 2003;38(1):91-6.

36. Masliah-Planchon J, Garinet S, Pasmant E. RAS-MAPK pathway epigenetic activation in cancer: miRNAs in action. Oncotarget. 2016;7(25):38892–907.

37. Peluso I, Yarla NS, Ambra R, Pastore G, Perry G. MAPK signalling pathway in cancers: Olive products as cancer preventive and therapeutic agents. Semin Cancer Biol. 2017;

38. Kim EK, Choi E-J. Compromised MAPK signaling in human diseases: an update. Arch Toxicol. 2015;89(6):867-82.

39. Lei Y-Y, Wang W-J, Mei J-H, Wang C-L. Mitogen-Activated Protein Kinase Signal Transduction in Solid Tumors. Asian Pacific J Cancer Prev. 2014;15(20):8539-48.

40. Vlashi E, Pajonk F. Cancer Stem Cells, Cancer Cell Plasticity and Radiation Therapy. Semin Cancer Biol. 2015;28-35.

41. Munro MJ, Wickremesekera SK, Peng L, Tan ST, Itinteang T. Cancer stem cells in colorectal cancer: a review. J Clin Pathol. 2018;71(2):110-6.

42. Dreesen O, Brivanlou AH. Signaling pathways in cancer and embryonic stem cells. Stem Cell Rev. 2007;3(1):7-17.

43. Zhao J, Fu Y, Wu J, Li J, Huang G, Qin L. The Diverse Mechanisms of miRNAs and lncRNAs in the Maintenance of Liver Cancer Stem Cells. Biomed Res Int. 2018;1-9.

TABLES

Gen	Sequences and TM°.
E-cadherin	Forward 5'-AGCAGAACTAACTAACACACACGGGG-3' 64.4°C; Reverse 3'-TGCAACGTCGTTACGAGTCA-5' 66°C
EpCAM	Forward 5'-AGATTCTTGGCAGCGGTTCT-3' 67.1°C; Reverse 3'-GTTCTGTACTCACCAGCACCAGCACAA-5' 67.6°C
Vimentina	Forward 5'-AAATGGGCTCGTCACCTTCGT-3' 66.1°C; Reverse 3'-TTGCGCTCCTGAAAAACTGC-5' 67.8°C
Snail	Forward 5'-AAGATGCACATCCGAAGCC-3' 68.2°C; Reverse 3'-TCATCAAAGTCCTGTGGGGC-5' 67.7°C

Table 1. Sequences of the primers for the molecular markers.

Tool	# genes
TaRBase (validated)	336
Micro-TDS (predicted)	1530
TargetScan (predicted)	908

Table 2. Number of predicted and validated genes for miR-137.

KEGG pathway	p-value	# of genes
Hippo signaling track	0.0001535201220	9
Extracellular matrix (ECM) receptor interaction.	0.0004011268832	5

Table 3. Analysis of miR-137-regulated pathways with Tarbase.

KEGG pathway	p-value	# of genes
MAPK signaling pathway	0.00978078453869	46
Pathways regulating pluripotency in stem cells	0.00978078453869	25
ErbB signaling pathway	0.0100563980343	20
Thyroid hormone signaling pathway	0.0100563980343	23
Hippo signaling track	0.0142207521344	26
Oxytocin signaling pathway	0.0142207521344	29
Calcium signaling pathway	0.0160605828591	33
Adherent joints	0.0160605828591	16
Signaling pathway cAMP	0.0436427752089	36
Focal adhesion	0.0436427752089	37

Table 4. Analysis of the pathways regulated by miR-137, using the 3 tools (Tarbase, micro-TDS and TargetScan).

FIGURES

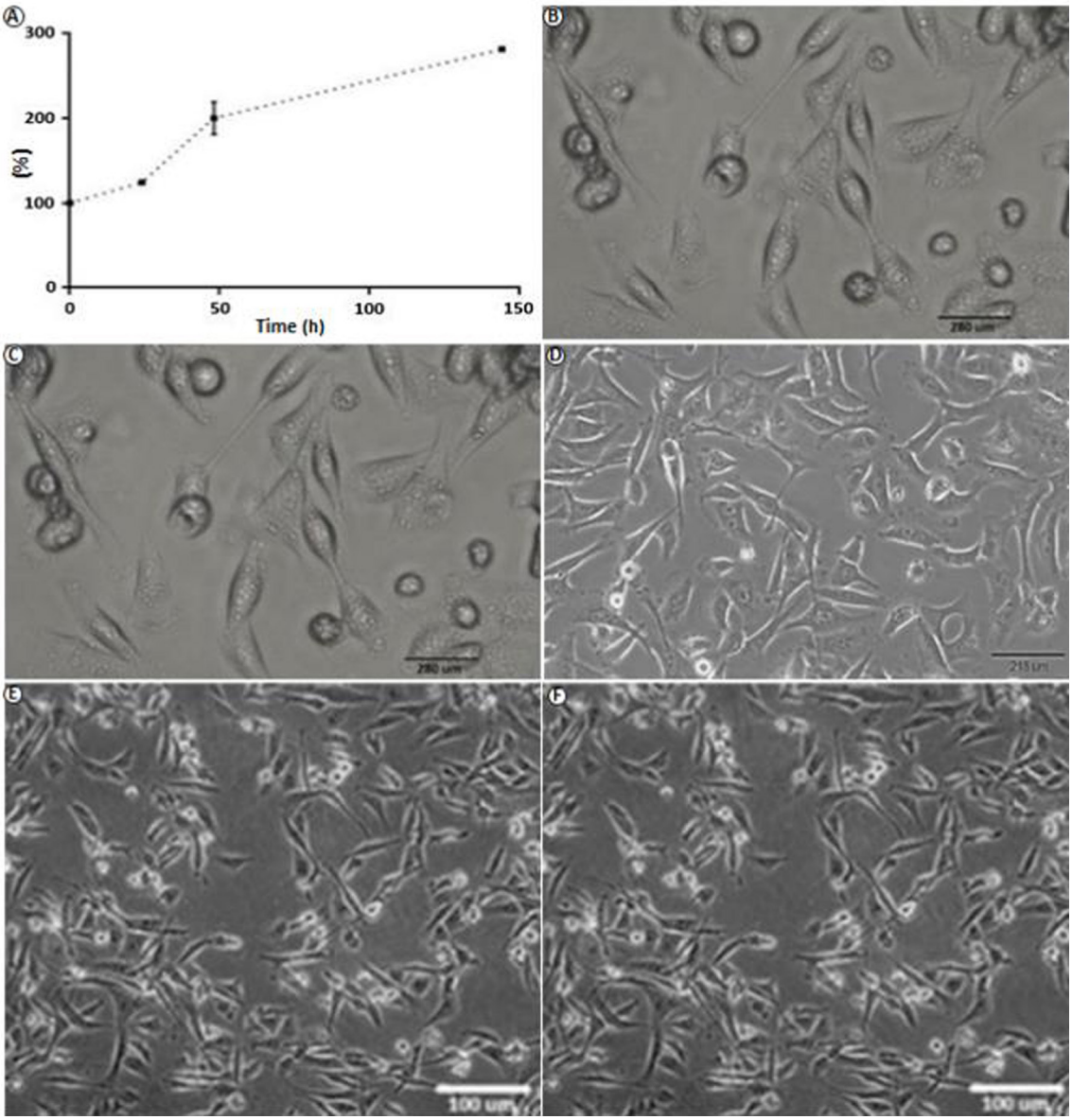

Figure 1. MDA-MB-231 cells. A) Cell growth at 24, 48, and 144 hours after seeding is shown. The graph shows the average ± SEM of 3 independent experiments. **B)** An image of the culture is shown, 20X (2 days of culture). **C)** The image shows the spindle-shaped phenotype of MDA-MB-231 cells, 4X (3 days of culture). **D)** Culture of MDA-MB-231 cells at 90% confluence is shown, 10X (5 days of culture). **E)** Image taken from ATCC and **F)** Image taken from Cahall (2015).

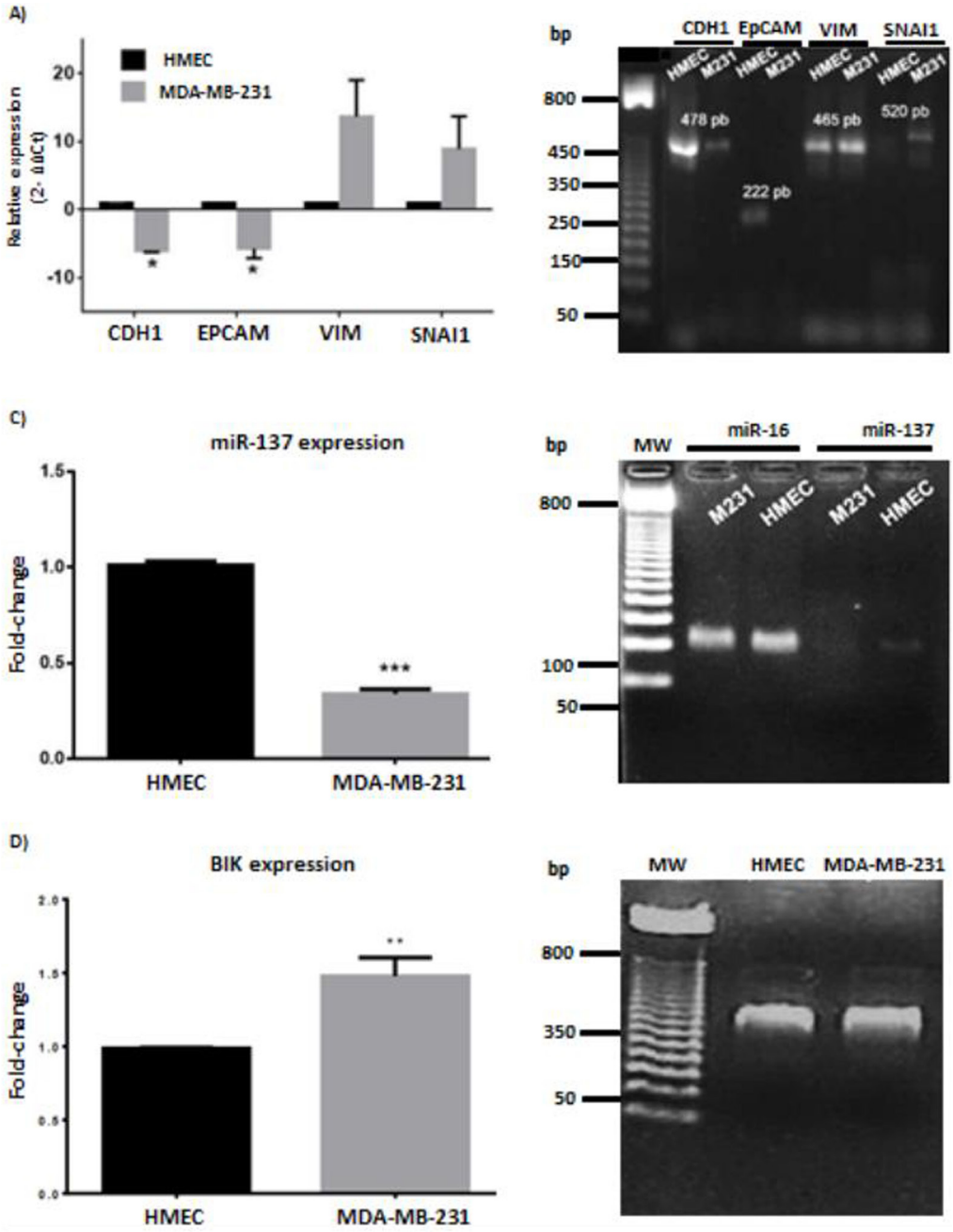

Figure 2. **mRNAs and miR-137 expression. A) qPCR.** Relative expression of epithelial (CDH1 and EPCAM) and mesenchymal (VIM AND SNAI1) markers determined by qPCR. The GAPDH gene was used to normalize the expression of each marker. Mean ± SEM of 3 independent experiments is shown. Statistical significance was determined by Student's *t* (*P < 0.05). The graph was generated with the GraphPad Prism V.6 software. For each gene amplified, agarose gels (2%) showed a single amplicon (MW (molecular weight marker) = 50-800 bp). This evidence and the Melt curve indicated the specificity of the reaction. **B) Relative miR-137 expression in the MDA-MB-231 cells**. The miR-16 was used to normalize expression. Mean ± SEM of 3 independent experiments is shown. Statistical significance was determined by Student's *t* (*P < 0.05). The graph was generated with GraphPad Prism V.6 software. An agarose gel (2%) shows the amplicons obtained for both miRNAs (100 bp amplicons; miScript SYBR® Green PCR kit). **C) Relative BIK expression in the MDA-MB-231 cells.** The GAPDH gene was used to normalize BIK expression. Mean ± SEM of 6 independent experiments is shown. Statistical significance was determined by Student's *t* (*P < 0.05). An **a**garose gel (2%) showing the amplicon obtained in the qPCR.

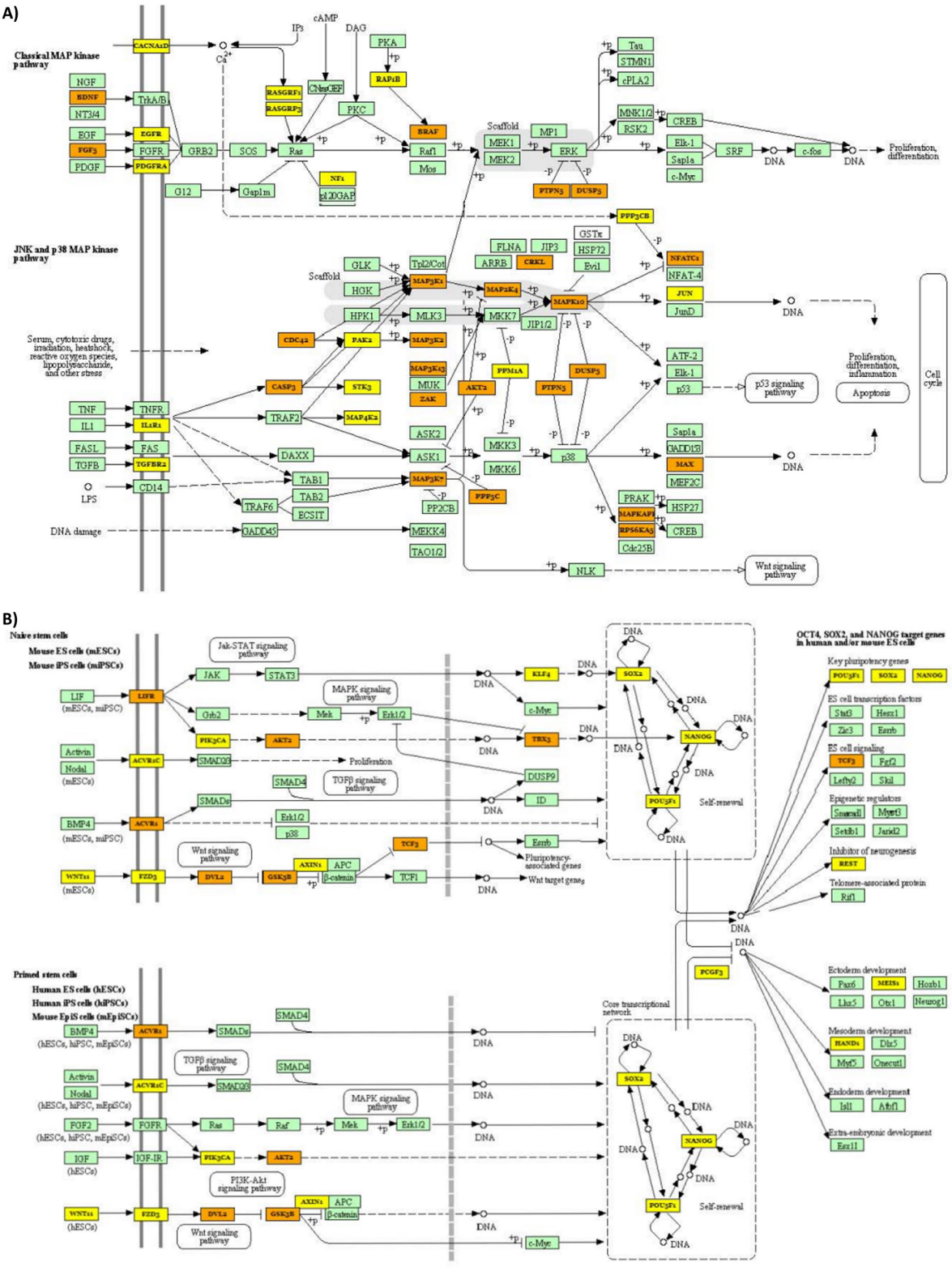

Figure 3. **DIANA-miRPath analysis**. The pathways potentially regulated by the miR-137 were identified from the validated and predicted genes using the Tarbase, micro-TDS and TargetScan tools. **A)** The MAPK pathway. **B)** Pluripotency-related pathways.

SUPLEMENTARY TABLES

ARPC5	FBXO42	FSTL1	LRRC58	WNT11	SHH
PIK3C3	PDZD2	HERC1	ADM	RPS27L	CLSTN1
RPA1	SEC23A	PHF10	TCEAL4	ZNF700	IRAQ1
IRS2	MCL1	ZNF770	SMCHD1	GAR1	NFIC
BRAF	DNAJB11	CANX	CSNK1A1	RANBP2	SOX2
PRLR	PNPLA6	PDS5A	CEBPA	SP1	BMP7
PAQR3	AKAP9	ABI3BP	SRPK1	SSR3	CTPS1
DARS2	MAP4	VPS13A	UQCRC2	FNIP1	RAD17
HIPK2	SNRK	CCT6A	UBE3C	SLC20A1	MAP3K7
ESYT1	HAND1	NAB1	SON	ZNF414	ITPR2
MFAP3	GOLGA8B	SOX21	MARCH8	FAM160B1	TET2
NFIX	STXBP5	CUL4A	PPM1A	AMOTL2	PCGF3
ATG7	MKRN2	TNRC6B	PALB2	PPARG	SLC40A1
UBE2Z	GPR180	PROX1	USP46	TMEM245	GOLGA3
G3BP1	PSPC1	STK39	PRKCSH	TP53BP1	PDHB
MASTL	RPL37	FAM20C	COL5A1	ATXN7L3B	GDPD1
FAM167A	ITGA5	GRN	MSH2	SELPLG	PFKFB4
ADAMTS5	ADO	AZIN1	CTSZ	PRPF4	MYL12A
EMP1	CCDC28A	LCAT	E2F6	MRPS6	CDC42EP2
EXT1	BCL11A	RYK	TFRC	UBE2G2	ENTPD7
LRP6	TNFRSF11A	RIOK2	SRPR	H3F3B	KPNB1
SMC1A	SELT	HECTD1	CEP350	ESRRA	PSMC1
UBP1	OSER1	FAM217B	ATRX	ZFR	SPOPL
RRAGD	DDX6	LAPTM4A	CSGALNACT1	HNRNPH1	SECISBP2L
UEVLD	MTIF2	ABCD3	TMEM131	CCNE1	TGFBR2
MED13L	RAB2A	AKT2	SNAPC4	NANOG	SLC1A5
UBE2Q2	IBTK	ARHGAP35	EIF4G1	CENPJ	EIF1
YAP1	NA	C9orf41	MIA3	GLIPR1	RAB14

GCLC	MARCH9	NPM1	TRIM33	PAPD7	ADRB1
FUS	MCFD2	PTGES2	TUBE1	PCMTD1	SGK1
FAM126B	MYO1C	ETNK1	PTGS2	LEPREL2	PSMB6
FABP4	MAN2A1	ITGAV	HECA	DNAJB12	MDM2
USP36	RNF217	ZNF385A	NCOA2	UPF2	SSR4
CBX2	USF2	ZFYVE16	CFL2	GOLGB1	RPL18
PPP1R9A	SETD5	TRAK2	BAZ2A	NSF	NT5DC1
MAST4	PPCS	CSE1L	MARCKSL1	TULP4	HOXC8
CENPT	FMR1	PMAIP1	NRP1	COG3	MYO1B
SIK3	PABPC4	OSBPL2	TMPO	UHMK1	PLS3
GRK5	TARDBP	KIAA1432	FXR1	TNRC6A	COQ7
MTHFD2	SMIM4	SMC4	DCUN1D3	BCMO1	ACO2
YWHAE	CLTC	SFXN1	JAZF1	OXR1	COL4A1
BTBD1	NOTCH2	SENP2	DDX5	RASAL2	DGKH
DENND4B	GLS	PIKFYVE	CUX1	ZBTB18	SNAP29
CALM3	LOX	RUNX1T1	XRN1	SNX6	PPP1CB
ZMYM4	TIMP2	AGO1	H3F3C	ALG13	FNIP2
COL12A1	ASPH	NECAP1	C6orf62	SLX4	ASAP2
THBS1	GRAMD3	PKP4	CDC42	PARD3	MEX3C
PTRF	CD2AP	BTG2	PMPCB	ATP2A2	ZCCHC3
ZNF267	RAB1A	CASP3	TMEM222	PAFAH1B2	NEFL
DBN1	SLC30A7	RNF4	IPO5	RPL35	OTUD7B
PRRC2B	HNRNPU	SSFA2	SCO1	ARHGEF7	GREM1
GAPDH	VLDLR	SBNO1	KCNC4	PLEKHA6	MOB1A
CTBP1	ZKSCAN8	GIGYF2	RPL28	ADK	ZC3H11A
KCNQ5	CDK6	NONO	CYSLTR1	AIMP2	AXL
YIPF6	KIF23	POU5F1	CCDC88A	CTDSPL2	PDIA6
VAC14	HEY2	SLC35C1	KCNK1	LEPROT	PITPNA

Supplementary Table S1. List of validated target genes for miR-137 (Tarbase).

KEGG Pathway	# of gene involved	GENES (ID)
ErB signaling pathway	15	TGFA EGFR NRG3 ERBB4 PIK3CA AKT2 GSK3B CRKL NCK2 PAK3 SRC MAP2K4 MAPK10 JUN BRAF
Thyroid hormone signaling pathway	19	ITGAV ATP1EA SLC16A10 THRE PIK3CA PLCB1 THRE KAT2B NCOSA1 MED27 ATP2A2 NOTCH1 GSK3B MDM2 TEC1D4 AKT2 PIK3CA SRC SLC16A10
Hippo signaling pathway	21	PARD3 YAP1 AJUEA LATS2 FRMD6 WWC1 STK3 MOE1A FRMD6 EMP7 WNT11 FZD3 YWHAE DVL2 GSK3B AXIN1 CTNNA3 SOX2 SNAI2 TEAD1 PPP1CE

Oxytocin signaling pathway	18	RYR3 PLCE1 CACNA1D KCNJ3 ADCY9 PIK3CA SRC ROCK1 PPP1CE ITPR2 CALM3 CAMKK2 CAMK2A PRKAE1 GUCY1A2 NFATC1 PTGS2 JUN
Calcium signaling pathway	22	SLC8A1 ATP2E2 ADRE1 CACNA1D CACNA1H GRIN2A HTR2C ERBB4 ADCY9 PLCE1 PLCZ1 STIM2 ATP2A2 RYR3 ITPR2 CALM3 SLC8A1 SLC25A5 PPP3CE CAMK2A ADCY1 PDE1A
Adherens junctions	19	PVRL3 PTPRB EGFR TGFBR2 CDC42 FER SRC ACTN2 TJP1 MAP3K7 SNAI2 SNA1 WASL CDC42 T2P3 CTNNA3 ACTN2 SSX2IP PARD3

cAMP signaling pathway	24	ADRE1 ADCY9 CMRM2 HCN2 CNGA1 CLAM3 CAMK2A ATP2B2 ATP1B1 GRIA4 GRIN2B RYR2 ATP2A2 ROCK1 MAPK10 RAP1E BRAF PDE4A AKT2 PPP1CE CREB5 NFATC1 BDNF JUN
Focal adhesions	19	COL4A1 ITGAV EGFR SRC ARHGAP3 CAPN2 PIK3CA PXN RASGRF1 CRKL AKT2 CDC42 PAK3 MAPK10 BRAF MYLL12A GSK3B JUN XIAP

Supplementary Table S2. Biologic pathways potentially regulated by the miR-137.